Rapid bottom-water circulation changes during the last glacial cycle in the coastal low-latitude NE Atlantic

David Gallego-Torres [a,b,], Oscar E. Romero [a], Francisca Martínez-Ruiz [a], Jung-Hyun Kim[c], Barbara Donner [d], Miguel Ortega-Huertas [b]

[a] Instituto Andaluz de Ciencias de la Tierra (CSIC-UGR), Avenida de las Palmeras 4, 18100 Armilla, Granada, Spain
[b] Departamento de Mineralogia y Petrologia (UGR), Facultad de Ciencias, Campus Fuentenueva, 18002 Granada, Spain
[c] NIOZ Royal Netherlands Institute for Sea Research, Department of Marine Organic Biogeochemistry, PO Box 59, AB Den Burg, 1790 Texel, The Netherlands
[d] MARUM—Center for Marine Environmental Sciences, University of Bremen, P.O. Box 330440, 28334 Bremen, Germany

Rapid bottom-water circulation changes during the last glacial cycle in the coastal low-latitude NE Atlantic

1. Introduction

Greenland ice core records show that climate ameriolation in the North Atlantic and surrounding regions was not smooth, but included a series of abrupt changes and reversals (e.g., Dansgaard et al., 1993; Grootes and Stuiver, 1997). Our understanding of rapid climate changes and the role played by the ocean circulation through heat and salinity redistribution remains still incomplete. One reason for this is the scarcity of suitable high sedimentation rate cores, containing appropriate proxy variables able to clearly solve the timing and phasing of atmospheric and ocean responses during abrupt climate reversals such as the Heinrich Events, Bølling-Allerød and Younger Dryas, undermining efforts to document the role played by ocean circulation during these events. The significance of oceans in globally redistributing heat and their ability to switch between different states of equilibrium has led to propose that changes in the Atlantic Meridional Overturning Circulation (AMOC), and associated modes of deep-water formation were responsible for the sharp climate shifts seen in Greenland ice core records (e.g., Rahmstorf, 2002). Several of these rapic AMOC shifts had a global imprint detected at different latitudes (Southern Iceland Rise (Thornalley et al., 2011) the Bermuda Rise (Hall et al., 2011; McManus et al., 2004), the Southern ocean (Rutberg et al., 2000)).

Due to its location in the easternmost border of the North Atlantic Subtropical Gyre, the upwelling system off Northwest Africa is very sensitive to variations of the AMOC (Kim et al., 2012). In addition to surface currents processes (Kim et al., 2012;

Romero et al., 2008), variations of deep-water conditions underlying this highly productive area are also recorded in downcore sediments (Filipsson et al., 2011). Hence, interpreting the record of both surface and deep water conditions as well as the possible effect of surface water productivity on the geochemical conditions at the sediment-water interface can deliver important insights for interpretating the local paleoceanographic setting and its possible extrapolation to other regions of the North Atlantic ocean.

Much attention has been paid to processes and mechanisms occurred during short-term Quaternary climate variations around the NW African region in the lower atmosphere (de Menocal et al., 2000a; de Menocal et al., 2000b; Kim et al., 2007; Kuhlmann et al., 2004), and the upper water column (Romero et al., 2008). However, much less is known about the bottom water processes affecting the sedimentary record. To assess variations of deep-sea conditions off Mauritania, we extend on Romero et al. (2008) and Filipsson et al. (2011) and reconstruct redox conditions and their significance for deep-water circulation during the last glacial cycle in the gravity core GeoB7926-2.

2. **Materials and Methods**

2.1 Core GeoB7926-2:

We present high-resolution records of bottom water conditions off Mauritania for the last glacial cycle, obtained from the gravity core GeoB7926-2, 1328cm length (20°13’N, 18°27’W, 2500 m water depth, Fig. 1).This core was recovered below the major upwelling region along the northwestern African continent (Romero et al., 2008). The Mauritanian shelf is generally narrow (about 45-55 km wide) and the continental slope is about 45 km wide with an average inclination of 2-3°. Numerous small and

several large canyons are located off the shelf edge (Futterer, 1983). Site GeoB7926-2 is ideally situated to monitor past variations in the climate and hydrography of northwest Africa, being on the confluence of different oceanic currents and within the latitudes of the Intertropical Convergence Zone (ITCZ). In this work, we present results for the depth interval between 113 and 803 cm (~10-24 kyr). The dominant lithology is foramifer-bearing nanofossil or diatom-ooze, with short intervals marked by clayey and quartz-bearing parts and a few turbidite layers in the upper 820 cm (Romero et al., 2008).

2.2 Stratigraphy:

The age control for the entire core GeoB7926-2 is based on 17 Accelerator Mass Spectrometry (AMS) ^{14}C dates determined on monospecific planktonic foraminifera *Globigerina inflata* (Leibniz Laboratory for Radiometric Dating and Stable Isotope Research, Kiel University, Germany), and the oxygen isotope record of the planktonic foraminifera *Globigerina bulloides*, (Kim et al., 2012; Romero et al., 2008). The ^{14}C ages were converted into calendar years using the CALIB REV6.0.0 program with the marine calibration dataset (MARINE09) (Stuiver et al., 1998). We used the mean ocean reservoir age of 400 kyr (Bard, 1988) although regional reservoir ages (ΔR) might be larger due to the upwelling of older subsurface waters (deMenocal et al., 2000b; Kim et al., 2012). We arbitrarily assumed similar changes in radiocarbon reservoir age throughout the studied interval though they might have varied through time. For instance, the marine ^{14}C reservoir age during the Younger Dryas was nearly twice as large as the modern value due to changes in deep ocean circulation and ocean atmosphere radiocarbon partitioning (deMenocal et al., 2000a; deMenocal et al., 2000b; Staubwasser et al., 2002). Based on this model, the main climatic phases are defined as follow: the Last Glacial Maximum (LGM) occurred between 23 and 19 kyr; Heinrich

74 Event 1 (HE1), 18 to 15.5 kyr; Bølling-Allerød (B-A), 15.5 to 13.5 kyr; Younger Dryas
75 (YD), 13.5 to 11.4 while the Holocene extended from 11.5 kyr onwards.

76 2.3 Geochemical Proxies:

77 Inorganic geochemistry record, as a whole, and trace element record in particular,
78 are scarce in the area off Mauritania. Martinez et al., (1999) provided the most reliable
79 Mo record tracing long term changes in redox conditions under this upwelling system.
80 However, no high resolution studies have been carried out to detect abrupt changes in
81 oceanographic conditions in the region. With the aim of obtaining a high resolution
82 record for the period between 25.0 and 10.0 kyr, trace elements contents were
83 determined by bulk sediment geochemical analyses and are used to reconstruct
84 oxygenation conditions of the depositional environment. Samples were dried and
85 ground in an agate mortar, homogenized for geochemical analyses and aliquots portions
86 were used to determine TOC and major and trace element concentrations. TOC
87 measurements were made at Bremen University, calculated as the difference between
88 carbon content of the total sample and carbon content after acidification (Romero et al.,
89 2008). Total dissolution of the sample was carried out using HF and HNO_3 following
90 the standard procedures for these samples described in *Gallego-Torres et al.* [2007]. Al,
91 Ca, K and Mn contents were determined by Atomic Absorption spectrometry at the
92 Analytical Facilities of the University of Granada (CIC) using Re and Rh as internal
93 standards. Trace elements (U and Mo) were measured with an ICP-MS Perkin-Elmer
94 Sciex Elan 5000 spectrometer (CIC). Coefficients of variation calculated by dissolution
95 and subsequent analyses of 10 replicates of powdered samples were better than 3% and
96 8% for analyte concentrations of 50 and 5 ppm respectively. , In order to correct for
97 detrital variations, all elements were normalized to Al content (Van Der Weijden,
98 2002).

99 Mo and U are used as redox proxies since they change their solubility and stability
100 depending on their redox state precipitating under reduced oxygen concentration and/or
101 in the presence of HS^- (Algeo and Tribovillard, 2009; Morford et al., 2009; Tribovillard
102 et al., 2006). U can precipitate under hypoxic conditions forming uraninite as a result of
103 Fe(II)-Fe(III) bacterial mediated redox boundary (Morford et al., 2009) whereas Mo
104 precipitates mainly as sulphides on presence of HS^- (Morford et al., 2005; Morford et
105 al., 2009) thus implying anoxic-sulphidic conditions (Fig. 2 E-F). Their co-variation,
106 expressed as enrichment factors (Arthur et al., 1990), provides information about
107 oxygenation in the water column and/or the evolution on the redox conditions and
108 chemistry of the basin (see Algeo and Tribovillard, 2009 for details). The studied area
109 should behave similarly to other upwelling areas where the average sea-water Mo/U
110 ratio can be considered as the "limiting budget" of Mo-U covariation provided that the
111 water column is neither anoxic nor stagnant throughout. Under these circumstances,
112 Mo/U seawater ratio represents the maximum rate of fixation meaning anoxic
113 environment at the sediment-water interface and the redoxcline being slightly above the
114 seafloor.

115 Opposite to these two elements, Mn precipitates as oxy-hydroxides in the presence
116 of free O_2 (Thomson et al., 1993). Diagenetic Mn concentration in the sediments
117 implies oxygen penetration in the sediment and precipitation of oxy-hydroxides when
118 downward diffusing O_2 encounters upwards diffusing dissolved Mn in pore waters from
119 underlying anoxic sediment column, allowing the reconstruction of re-oxygenation
120 events (Gallego-Torres et al., 2010; van Santvoort et al., 1996).

121 K and Ca are used to detect changes in the sedimentary regime. Ca can be
122 quantified as CO_3Ca, thus related to calcareous organism, although a calcite
123 preservation effect must be considered, and K is mainly derived from detrital material

(illite and other clay minerals, and feldspars). Total primary productivity is interpreted from C_{org} content and C_{org} AR (Romero et al., 2008).

3. Results

Organic matter deposition is represented as C_{org} content and C_{org} accumulation rate (AR) on Figure 2 A and B. C_{org} show minimum values during early HE1 and high concentration in the LGM and YD. C_{org}AR is maximum during the YD, also showing high values during the early deglaciation (~19-17 kyr) and early HE1 (~13-11.5 kyr).

K/Al ratio shows high values during the LGM with a sharp decrease coinciding with the onset of the deglaciation (Fig. 2 C). A progressive increase until the early HE1 is followed by low K/Al ratio from 17.0 to 15.5 kyr. The B-A is characterized by high K/Al at the onset and a steep decrease, whereas high values define the YD. Ca/Al ratio presents generally low values during LGM (Fig. 2 D) progressively increasing until the early HE1. The later part of this event presents relatively low values while the warm B-A period exhibit high Ca/Al ratio. The YD presents low Ca/Al similar to LGM values.

Figure 3 shows Mo to U co-variation expressed as enrichment factors. Most of the values remain below average oceanic Mo/U ratio (grey line) (Algeo and Tribovillard, 2009) and only during the YD this ratio reaches the seawater threshold.

Redox sensitive elements profiles are also presented on Fig. 2. Almost constant low values of Mo/Al (Fig. 2 E) and U/Al (Fig. 2 F) are observed throughout the LGM. A minor increase for Mo and U is recorded around 22.3kyr. Preferential Mn precipitaion characterizes the period between 19 and 17 kyr. Overlying this Mn peak, Mo/Al and U/Al progressively increases until the onset of HE1, when a sharp peak of both ratios is recorded. Low Mo concentration and generally lower though fluctuating U/Al ratios are

observed during the B-A, whereas the YD event is again characterized by high Mo and U with a sharp Mn increase around 12.3kyr. After the YD, around 11kyr, low Mo, U and Mn values characterize the transition toward the early Holocene.

4. Discussion

4.1 Bottom water oxygenation off Mauritania during the last deglaciation

Low C_{org} AR (Fig. 2B) evidence that productivity was relatively low during the early part of the LGM (Romero et al., 2008). The dominance of silicate-poor North Atlantic Central Waters (NACW) bathing the upwelling area off Mauritania might have limited diatom production at the time, whereas calcareous organisms, as shown by Ca values (Fig. 2D), contributed the most to productivity in surface waters (Romero et al., 2008) . Later in LGM, Ca content decreased and higher C_{org} occurred, but AR remains constant. More corrosive bottom waters, such as Antartic Bottom Waters (AABW) (Lippold et al., 2012) might enhanced carbonate dissolution. Very low content of Mo and U (Fig. 2) indicates high content of O_2 dissolved in deep-water masses as well as downward diffusion into the upper section of the sediment column. This implies that ventilation of the deep-water mass off Mauritania at 2500m was efficient enough to maintain oxic conditions at the sediment-water interface throughout the LGM.

It has been argued that changes in oceanic circulation of the North Atlantic during the LGM affected mainly surface and intermediate waters (Lynch-Stieglitz et al., 2007), allowing upwelling of silica-rich waters and enhancing diatom productivity during the latest LGM and the transition into the glacial termination (see Romero et al., 2008). Deep-water circulation, on the other hand, remained strong throughout the late LGM and the onset of the deglaciation (McManus et al., 2004) allowing the good oxygenation

of the sea bottom at site GoB7926, as evidenced by low trace metal content (Fig. 2G-F), although deep water masses might have also changed from northerly sourced waters to southern origin (AABW).

A strong decrease in C_{org} content (Fig. 2A) characterizes the early stage of the deglaciation. Higher C_{org} AR, however, suggests a possible dilution effect related to higher calcareous production (Romero et al., 2008). Ca content progressively increased (Fig. 2D) together with detrital material delivery reflected by increasing K/Al ratio (Fig. 2C). Between the early deglaciation and the onset of HE1, the enhanced Mn precipitation indicates the occurrence of an oxidation front within the sediment, which might have partially degraded organic matter, similar to the process described for eastern Mediterranean sapropels (e.g., de Lange and Ten Haven, 1983; Gallego-Torres et al., 2010). At site GeoB7926, however, this phenomenon occurred in an hemipelagic basin with much higher accumulation rate than those recorded in the eastern Mediterranean Sea. Two conclusions can be extracted from the occurrence of this oxidation front: on one hand, the amount of C_{org} accumulated must have been greater than presently measured at site GeoB7926 (e.g., Thomson et al., 1995), while deep-water ventilation, as shown by high Mn and also low U and Mo concentrations (Fig. 2), must have been strong enough to keep oxic conditions at the sediment-water interface,. After the LGM, organic matter might have been more efficiently transported and accumulated due to high sedimentation rate at site GeoB7926 (Romero et al., 2008); simultaneously, as suggested by the spiky signal of C_{org}, U/Al and Mn/Al between 18.0 kyr and 17.3 kyr (Fig. 2), high bottom-water ventilation allowed the partial oxidation of the deposited organic carbon.

The first shift event in redox conditions corresponds to the late HE1 (~16 kyr). Intensified NE trade winds characterized the end of HE1 off Mauritania (Filipsson et al.,

2011), which favored upwelling and diatom productivity in surface waters (Romero et al., 2008). C_{org} content during the late HE1 (~16 kyr) is higher while C_{org} AR is lower than immediately before (19-17 kyr), hence resembling LGM values. Although it was not the only factor inducing high C_{org} values, the origin of the organic matter accumulated in the sediments and the composition of the diatom assemblage (Romero et al., 2008) might have played an important role in C_{org} accumulation in the sediment. Values of precipitated Mo and U (Fig. 2E-F) indicate that sub-oxic to anoxic conditions ruled at the sediment-water interface during second half of HE1. Water column stagnation is very unlikely in this oceanic setting, albeit both Mo/Al and U/Al profiles evidence reducing conditions in bottom sediments from 16.5 through 15 kyr. Additional support to this scenario is provided by the dominance of the benthic foraminifera *Bulimina exilis* at GeoB7926 between 17 and 15kyr, interpreted as evidence for reduced oxygen conditions at the seafloor (Filipsson et al., 2011). Intense export productivity could have lead to the consumption of most of the dissolved oxygen in bottom waters, hence inducing anoxia at the sediment-water interface and the uppermost sediment column. However, C_{org} AR during the late HE1 remained relatively low (<0.5gr/cm^2/kyr) compared with previous phases; during the interval between 19kyr-17.3 kyr C_{org}AR raised up to 1.0gr/cm^2/kyr (Romero et al., 2008), although no precipitation of Mo nor U indicates suboxic conditions. During the HE1 the situation is opposite; no dramatic increase in C_{org} AR and high Mo and U precipitation. Hence, we invoke reduced ventilation, thus slower deep-water currents, during this period.

The relatively warm B-A (15.5-13.5 kyr) experienced an important shift in the composition of the producers community in surface waters, favoring the primary production of calcareous over siliceous organisms (Romero et al., 2008). Since AR remained constant throughout the B-A (Fig. 2) changes in C_{org} content indicate varying

degradation of organic matter. Mo/Al values evidences mostly well oxygenated bottom waters, although the "background" content is higher than both during the LGM and present day conditions (Martinez et al., 1999). On the other hand, U fixation at site GeoB7926 was relatively high and fluctuated intensively (Fig. 2F). Since U precipitates before Mo in the transition from oxic to anoxic conditions (Algeo and Tribovillard, 2009; Tribovillard et al., 2006), the comparison of both parameters indicates slightly reduced oxygen availability in bottom waters over site GeoB7926, despite the fact that no HS^- was present neither in bottom waters nor in the uppermost sediment layer. Accordingly, *Thornalley et al*. (2011) described restricted ventilation during short duration cold spells occurring during the B-A. We argue that the resumption of strong deep-water circulation (and possibly ventilation) was not complete during the B-A and thus the redox boundary was, at least intermittently, very close to the sediment-water interface at site GeoB7926. This is additionally supported by low Mn values (Fig. 2G) which indicate that neither Mn was diffusing (upwards) nor O_2 was penetrating deep enough into the sediment.

The YD (13.5-11.5kyr) represents a return to paleoceanographic bottom water conditions similar to those recorded during the HE1, though this time dissolved oxygen deficiency was more severe. Maxima in trace element fixation, (Fig. 2E and F), hence very low oxygen content at the sea bottom, was also accompanied by high C_{org} AR related to increased diatom productivity (Romero et al., 2008) . The sharp decrease in carbonate sedimentation and the increase in detrital material at the early YD, shown by enhanced values of K/Al, led to high sedimentation rate, thus low C_{org} content during this early phase is possibly due to dilution occurred at site GeoB7926. However, the progressive rise in diatom productivity in surface waters (Romero et al., 2008) lead to an increase in C_{org} content and C_{org} AR, and reduced oxygen availability at the sea-floor

(Filipsson et al., 2011). This is further demonstrated by the geochemical signal at site GeoB7926. Mo/Al and U/Al reach maximum values while their covariation evidences minimum bottom water oxygenation; data points corresponding to the YD (Fig. 3 black diamonds) plot along the mean seawater Mo/U line, indicating maximum rate of fixation of Mo and U, similar to the scenario described by Algeo and Tribovillard (2009) for other upwelling areas suffering bottom water anoxia. All these geochemical signals evidence that restricted deep water circulation ruled during this cold interval. However, in addition to deep-water restriction, strongly increased diatom productivity in surface waters added its effect to induce bottom water anoxia. Enhanced export productivity implied intense oxygen consumption accelerating Mo and U fixation in the sediment (Fig. 2E-F). On the other hand, our Mn/Al profile (Fig. 2G) evidences Mn precipitation typical of oxidation fronts in the sediment column (de Lange, 1992; Froelich et al., 1979), indicative of an event of O_2 enrichment in bottom waters flowing upon the area. While high productivity conditions still occurred in surface waters overlying site GeoB7926, deep-water ventilation was temporarily resumed at the seafloor during the YD. The core recovery water depth is around the area of maximum Mn precipitation (e.g., de Lange et al., 2008) and thus short increases of O_2 concentration in bottom waters would allow a certain, though depth-limited penetration of the oxidation front inducing Mn precipitation. This process would also partially oxidize deposited organic material, explaining the spiky signal of the C_{org} profile during the YD. Thus, a pulse of highly oxygenated deep-water flowed over site GeoB7926, although poorly ventilated seafloor was the rule during the YD. After this cold phase, deep-water oxic conditions were reestablished in off Mauritania, remaining stable throughout the Holocene (Martinez et al., 1999).

4.2 Deep-water masses circulation in the coastal northeastern Atlantic

The discussed scenarios of bottom waters oxygenation and ventilation conditions are compared with other published $^{231}Pa/^{230}Th$ records (Gherardi et al., 2005; Lippold et al., 2012; McManus et al., 2004) shown in Fig. 4. The cores used for such comparison are scattered across the North Atlantic (Fig. 1). Although the use of $^{231}Pa/^{230}Th$ record has been under debate in the the North Atlantic eastern margin, Lippold et al, (2012) proved its reliability on core GeoB9508-5, located close to our studied site. This comparison allows us to propose five phases of different deep-water masses circulation off Mauritania summarized on Table 1.

1) During the LGM, deep-water circulation must have been more intense than later during the deglaciation. Although *Marchal et al.* (2000) suggested a decrease of almost 40% in AMOC, *McManus et al*. (2004) pointed towards a weak slowdown, while *Zhao et al.* (2000) proposed intensified effect of highly oxygenated AABW flowing northwards. Our interpretation of intense ventilation and O_2 availability is coherent with this later scenario and low Ca content is also consistent with north-flowing more corrosive AABW (Lippold et al., 2012). Glacial conditions induced restricted North Atlantic advection allowing AABW to flow northwards in the deeper layers.

2) The first stage of the deglaciation (~19.0 to 18.5 kyr) records no noticeable change in redox conditions (Fig. 2E-F). The transition between the LGM and HE1 is thought to have experienced circulation conditions very similar to those of the present-day (McManus et al., 2004) and thus this period represents the shift from AABW (Zhao et al., 2000) to NADW flowing between 1700 and 2500m depth (Gherardi et al., 2005; Mittelstaedt, 1991), the deepest value corresponding to the water depth where core GeoB7926 was retrieved.

3) Although HE1 event was a cold spell, it is unlikely that AABW (flowing below 4000m depth (Gherardi et al., 2005; Sarnthein et al., 1981) was able to push up to 2500m depth in such a short time interval. In addition, sub-oxic conditions observed during this period (Fig. 2F) are not consistent with the flow of well-oxygenated AABW. Instead, the slowdown of the deep North Atlantic circulation is a more plausible explanation. The collapse of the AMOC between 17.5 and 15kyr (McManus et al., 2004) matches with striking precision with the top and bottom of the Mo/Al peak at GeoB7926-2 (yellow highlight, Fig. 2E; Fig. 4c). Therefore, we propose that the slowdown of the AMOC weakened or even prevented regular circulation in the deeper layers of the coastal NE Atlantic (Table 1) and decreased the ventilation rate at the seafloor (Filipsson et al., 2011), while high productivity still occurred at surface waters (Romero et al., 2008).

4) Warmer SST during the B-A period at site GeoB7926 (Romero et al., 2008) coincides with relatively well oxygenated bottom waters. *McManus et al.* (2004) proposed that the AMOC resumed during the B/A, alas their $^{231}Pa/^{230}Th$ record shows slightly higher values than present-day ones (McManus et al., 2004), pointing to a less efficient AMOC. Likewise, Gherardi et al., (2005) proposed slower deep-water circulation than nowadays at both eastern and western margins of the North Atlantic during the B-A. Our results agree with both authors observations and support our interpretation at site GeoB7926 (Fig. 4 and Table 1). Reconstructed warmer conditions during the B-A off Mauritania (Kim et al., 2012; Romero et al., 2008) were accompanied by the resumption of deep-water circulation, though intermittent cold spells (Thornalley et al., 2011) induced less efficient oxygenation than during the interval immediately before HE1.

5) The low O_2 availability at site GeoB7926 records the repeated collapse of the AMOC along the NW African margin during the YD. Reducing conditions were helped by very intense surface productivity forcing O_2 consumption by this excess of exported organic matter (Filipsson et al., 2011). During the YD, the slowdown of the AMOC in the North Atlantic was not as intense as during HE1 (McManus et al., 2004). Schmidt and Lynch-Stieglitz (2011) also recorded the synchronicity of North Atlantic circulation and atmospheric conditions during the YD based on foraminifera shell composition from a core recovered on the Florida Strait (Fig. 4b). Benthic foraminifera record from a core south of Iceland, *Thornalley et al.* (2011) show that the YD, although globally characterized by a decrease in deep ocean ventilation (Gherardi et al., 2005; McManus et al., 2004), was interrupted by a moderate ventilation event between 12.6 and 12.1kyr. This ventilation event is also recorded on core GeoB7926 as a Mn oxidation front in between the suboxic phase marked by Mo and U. Thus, the signals of AMOC collapse and resumption during the YD described on the studied core are easily correlated with different records across the North Atlantic, reinforcing our interpretation and extending the reconstruction of AMOC circulation towards the East African margin.

5. Conclusions

We highlight the importance of the geochemical record off-Mauritania for the reconstruction of deep-water paleoceanography and the implication on North Atlantic Ocean circulation.

Deep-water oxygenation at site GeoB7926 is interpreted in combination with paleoproductivity in order to reconstruct a balance between oxygen consumption due to enhanced export productivity and decreased bottom water ventilation.

Two main phases of decreased ventilation are recognized off Mauritania; HE1 and YD, both matching with cold spells that prevented normal AMOC (Gherardi et al., 2005; McManus et al., 2004).

We confirm that the phases of AMOC collapse already recorded for the western part of the low-latitude Atlantic (McManus et al., 2004) are also recognizable in the eastern part of the Northeastern Atlantic, further supporting the shifts of North Atlantic circulation in the eastern basin.

Acknowledgements

We thank funding by 2008-00050084447 (Ministerio de Medioambiente y del Medio Rural y Marino), CGL2009-07603 (Ministerio de Ciencia y Tecnología), project P09-RNM-5212 (Junta de Andalucia) and Research Group RNM 0179 (Junta de Andalucia). We also thank the Centro de Instrumentación Científica (Universidad de Grananda, Spain), for analytical support. O.E.R. was partially supported by the Spanish Council of Scientific Research.

REFERENCES

Algeo, T. J., and Tribovillard, N. (2009). Environmental analysis of paleoceanographic systems based on molybdenum-uranium covariation. *Chemical Geology* **268,** 211-225.

Arthur, M. A., Brumsack, H.-J., Jenkyns, H. C., and Schlanger, S. O. (1990). Stratigraphy, geochemistry, and paleoceanography of organic carbon-rich Cretaceous sequences. *In* "Cretaceous Resources, Events and Rhythms." (R. N. Ginsburg, and B. Beauoin, Eds.), pp. 75-119. Kluwer, Dordrecht.

Bard, E. (1988). Correction of Accelerator Mass Spectrometry 14C Ages Measured in Planktonic Foraminifera: Paleoceanographic Implications. *Paleoceanography* **3,** 635-645.

Dansgaard, W., Johnsen, S. J., Clausen, H. B., Dahl-Jensen, D., Gundestrup, N. S., Hammer, C. U., Hvidberg, C. S., Steffensen, J. P., SveinbjÃ¶rnsdottir, A. E., Jouzel, J., and Bond, G. (1993). Evidence for general instability of past climate from a 250-kyr ice-core record. *Nature* **364,** 218-220.

de Lange, G. J. (1992). Distribution of exchangeable, fixed, organic and total nitrogen in interbedded turbiditic/pelagic sediments of the Madeira Abyssal Plain, eastern North Atlantic. *Marine Geology* **109,** 95-114.

de Lange, G. J., and Ten Haven, H. L. (1983). Recent sapropel formation in the Eastern Mediterranean. *Nature* **305,** 797-798.

de Lange, G. J., Thomson, J., Reitz, A., Slomp, C. P., Principato, M. S., Erba, E., and Corselli, C. (2008). Synchronous basin-wide formation and redox-controlled preservation of a Mediterranean sapropel. *Nature Geoscience* **1,** 606-610.

de Menocal, P., Ortiz, J., Guilderson, T., Adkins, J., Sarnthein, M., Baker, L., and Yarusinsky, M. (2000a). Abrupt onset and termination of the African Humid Period: Rapid climate responses to gradual insolation forcing. *Quaternary Science Reviews* **19,** 347-361.

de Menocal, P., Ortiz, J., Guilderson, T., and Sarnthein, M. (2000b). Coherent high- and low-latitude climate variability during the holocene warm period. *Science* **288,** 2198-2202.

deMenocal, P., Ortiz, J., Guilderson, T., Adkins, J., Sarnthein, M., Baker, L., and Yarusinsky, M. (2000a). Abrupt onset and termination of the African Humid Period: Rapid climate responses to gradual insolation forcing. *Quaternary Science Reviews* **19,** 347-361.

deMenocal, P., Ortiz, J., Guilderson, T., and Sarnthein, M. (2000b). Coherent high- and low-latitude climate variability during the holocene warm period. *Science* **288,** 2198-2202.

Filipsson, H. L., Romero, O. E., Jan-Berend, W. S., and Donner, B. (2011). Relationships between primary productivity and bottom-water oxygenation off northwest Africa during the last deglaciation. *Journal of Quaternary Science* **26,** 448-456.

Froelich, P. N., Klinkhammer, G. P., Bender, M. L., Luedtke, N. A., Heath, G. R., Cullen, D., Dauphin, P., Hammond, D., Hartman, B., and Maynard, V. (1979). Early oxidation of organic matter in pelagic sediments of the eastern equatorial Atlantic: suboxic diagenesis. *Geochimica et Cosmochimica Acta* **43,** 1075-1090.

Futterer, D. K. (1983). The modern upwelling record off northwest Africa. *In* "Coastal Upwelling, Its Sediment Record. Part B: Sedimentary records of Ancient Coastal Upwelling." (S. Thiede J., E., Ed.), pp. 105-121. Plenum, New York.

Gallego-Torres, D., Martinez-Ruiz, F., De Lange, G., Jimenez-Espejo, F. J., and Ortega-Huertas, M. (2010). Trace-elemental derived paleoceanographic and paleoclimatic conditions for Pleistocene Eastern Mediterranean sapropels. *Palaeogeography Palaeoclimatology Palaeoecology* **293,** 76-89.

Gherardi, J. M., Labeyrie, L., McManus, J. F., Francois, R., Skinner, L. C., and Cortijo, E. (2005). Evidence from the Northeastern Atlantic basin for variability in the rate of the

meridional overturning circulation through the last deglaciation. *Earth and Planetary Science Letters* **240,** 710-723.

Grootes, P. M., and Stuiver, M. (1997). Oxygen 18/16 variability in Greenland snow and ice with 10-3- to 105-year time resolution. *Journal of Geophysical Research* **102,** 26455-26470.

Hall, I. R., Evans, H. K., and Thornalley, D. J. R. (2011). Deep water flow speed and surface ocean changes in the subtropical North Atlantic during the last deglaciation. *Global and Planetary Change* **79,** 255-263.

Kim, J. H., Meggers, H., Rimbu, N., Lohmann, G., Freudnethal, T., MÃ¼ller, P. J., and Schneider, R. R. (2007). Impacts of the North Atlantic gyre circulation on Holocene climate off northwest Africa. *Geology* **35,** 387-390.

Kim, J. H., Romero, O. E., Lohmann, G., Donner, B., Laepple, T., Haam, E., and Sinninghe Damste, J. S. (2012). Pronounced subsurface cooling of North Atlantic waters off Northwest Africa during Dansgaard-Oeschger interstadials. *Earth and Planetary Science Letters* **339-340,** 95-102.

Kuhlmann, H., Meggers, H., Freudenthal, T., and Wefer, G. (2004). The transition of the monsoonal and the N Atlantic climate system off NW Africa during the Holocene. *Geophysical Research Letters* **31,** 1-4.

Lippold, J., Mulitza, S., Mollenhauer, G., Weyer, S., Heslop, D., and Christl, M. (2012). Boundary scavenging at the East Atlantic margin does not negate use of 231Pa/230Th to trace Atlantic overturning. *Earth and Planetary Science Letters* **333-334,** 317-331.

Lynch-Stieglitz, J., Adkins, J. F., Curry, W. B., Dokken, T., Hall, I. R., Herguera, J. C., Hirschi, J. J. M., Ivanova, E. V., Kissel, C., Marchal, O., Marchitto, T. M., McCave, I. N., McManus, J. F., Mulitza, S., Ninnemann, U., Peeters, F., Yu, E. F., and Zahn, R. (2007). Atlantic meridional overturning circulation during the last glacial maximum. *Science* **316,** 66-69.

Marchal, O., FranÃ§ois, R., Stocker, T. F., and Joos, F. (2000). Ocean thermohaline circulation and sedimentary 231PA/230Th ratio. *Paleoceanography* **15,** 625-641.

Martinez, P., Bertrand, P., Shimmield, G. B., Cochrane, K., Jorissen, F. J., Foster, J., and Dignan, M. (1999). Upwelling intensity and ocean productivity changes off Cape Blanc (northwest Africa) during the last 70,000 years: Geochemical and micropalaeontological evidence. *Marine Geology* **158,** 57-74.

McManus, J. F., Francois, R., Gherardl, J. M., Kelgwin, L., and Drown-Leger, S. (2004). Collapse and rapid resumption of Atlantic meridional circulation linked to deglacial climate changes. *Nature* **428,** 834-837.

Mittelstaedt, E. (1991). The ocean boundary along the northwest African coast: Circulation and oceanographic properties at the sea surface. *Progress in Oceanography* **26,** 307-355.

Morford, J. L., Emerson, S. R., Breckel, E. J., and Kim, S. H. (2005). Diagenesis of oxyanions (V, U, Re, and Mo) in pore waters and sediments from a continental margin. *Geochimica Et Cosmochimica Acta* **69,** 5021-5032.

Morford, J. L., Martin, W. R., FranÃ§ois, R., and Carney, C. M. (2009). A model for uranium, rhenium, and molybdenum diagenesis in marine sediments based on results from coastal locations. *Geochimica et Cosmochimica Acta* **73,** 2938-2960.

Rahmstorf, S. (2002). Ocean circulation and climate during the past 120,000 years. *Nature* **419,** 207-214.

Romero, O. E., Kim, J. H., and Donner, B. (2008). Submillennial-to-millennial variability of diatom production off Mauritania, NW Africa, during the last glacial cycle. *Paleoceanography* **23**.

Rutberg, R. L., Hemming, S. R., and Goldstein, S. L. (2000). Reduced North Atlantic Deep Water flux to the glacial Southern Ocean inferred from neodymium isotope ratios. *Nature* **405,** 935-938.

Sarnthein, M., Tetzlaff, G., Koopmann, B., Wolter, K., and Pflaumann, U. (1981). Glacial and interglacial wind regimes over the eastern subtropical Atlantic and North-West Africa. *Nature* **293,** 193-196.

Schmidt, B. C., and Lynch-Stieglitz, J. (2011). Florida Straits deglacial temperature and salinity change: Implications for tropical hydrologic cycle variability. *Paleoceanography* **26,** PA4205.

Staubwasser, M., Sirocko, F., Grootes, P. M., and Erlenkeuser, H. (2002). South Asian monsoon climate change and radiocarbon in the Arabian Sea during early and middle Holocene. *Paleoceanography* **17,** 15-1.

Stuiver, M., Reimer, P. J., Bard, E., Beck, J. W., Burr, G. S., Hughen, K. A., Kromer, B., McCormac, G., Van Der Plicht, J., and Spurk, M. (1998). INTCAL98 radiocarbon age calibration, 24,000-0 cal BP. *Radiocarbon* **40,** 1041-1083.

Thomson, J., Higgs, N. C., Croudace, I. W., Colley, s., and Hydes, D. J. (1993). Redox zonation of elements at an oxic/postoxic boundary in deep-sea sediments. *Geochemical and Comochimical Acta* **57,** 579-595.

Thomson, J., Higgs, N. C., Wilson, T. R. S., Croudace, I. W., De Lange, G. J., and Van Santvoort, P. J. M. (1995). Redistribution and geochemical behaviour of redox-sensitive elements around S1, the most recent eastern Mediterranean sapropel. *Geochimica et Cosmochimica Acta* **59,** 3487-3501.

Thornalley, D. J. R., Elderfield, H., and McCave, I. N. (2011). Reconstructing North Atlantic deglacial surface hydrography and its link to the Atlantic overturning circulation. *Global and Planetary Change* **79,** 163-175.

Tribovillard, N., Algeo, T. J., Lyons, T., and Riboulleau, A. (2006). Trace metals as paleoredox and paleoproductivity proxies: An update. *Chemical Geology* **232,** 12-32.

Van Der Weijden, C. H. (2002). Pitfalls of normalization of marine geochemical data using a common divisor. *Marine Geology* **184,** 167-187.

van Santvoort, P. J. M., de Lange, G. J., Thomson, J., Cussen, H., Wilson, T. R. S., Krom, M. D., and Strohle, K. (1996). Active post-depositional oxidation of the most recent sapropel (S1) in sediments of the eastern Mediterranean Sea. *Geochimica et Cosmochimica Acta* **60,** 4007-4024.

Zhao, M., Eglinton, G., Haslett, S. K., Jordan, R. W., Sarnthein, M., and Zhang, Z. (2000). Marine and terrestrial biomarker records for the last 35,000 years at ODP site 658C off NW Africa. *Organic Geochemistry* **31,** 919-930.

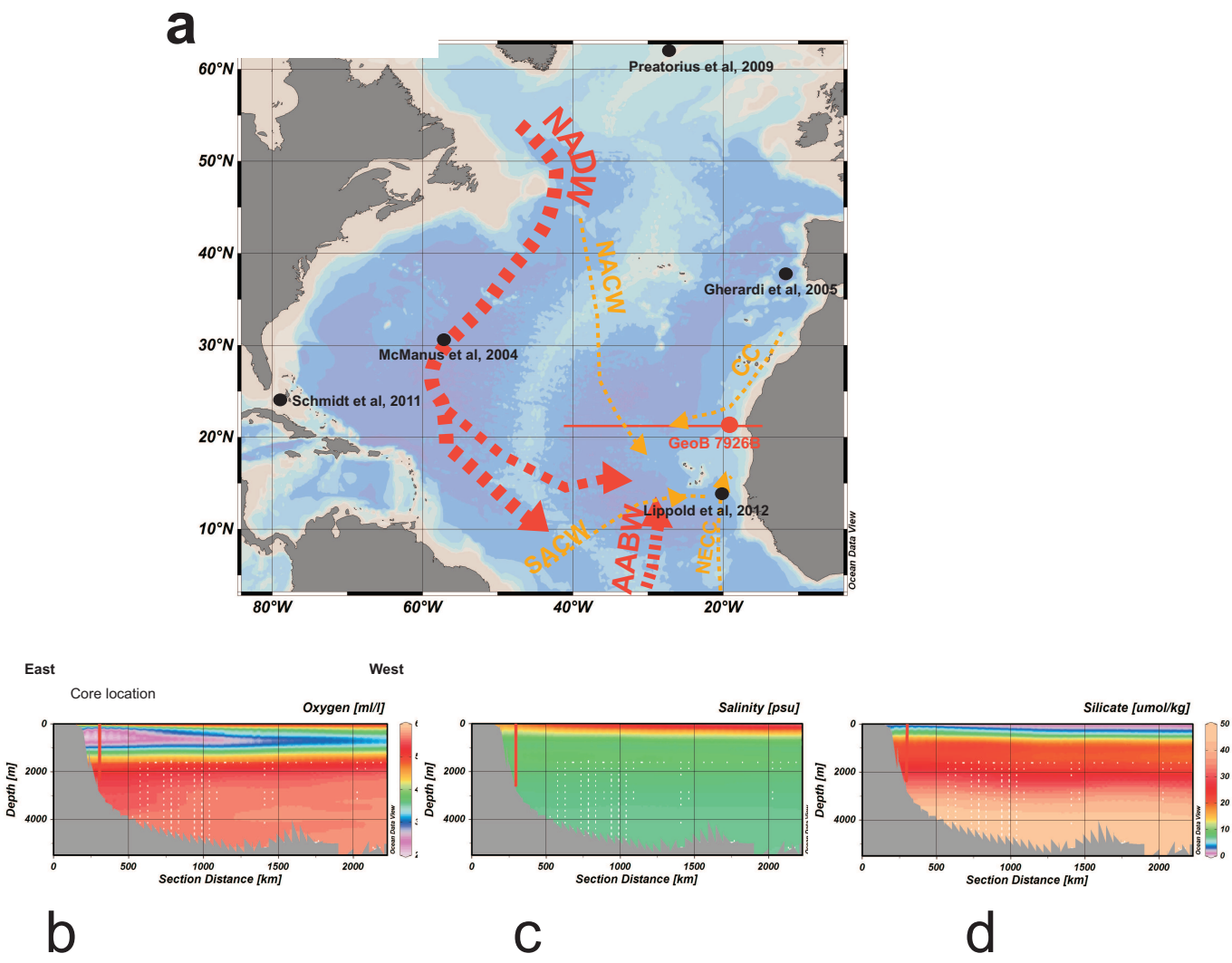

Figure 1. a) North Atlantic Deep Water (NADW); Antartic Bottom Water (AABW);North Atlantic Central Water (NACW); South Atlantic Central Water (SACW); Canary Current (CC); North Equatorial Counter Current (NECC). b) Water column disolved oxygen profile. c) Water column salinity profile. d) Water column silicate profile

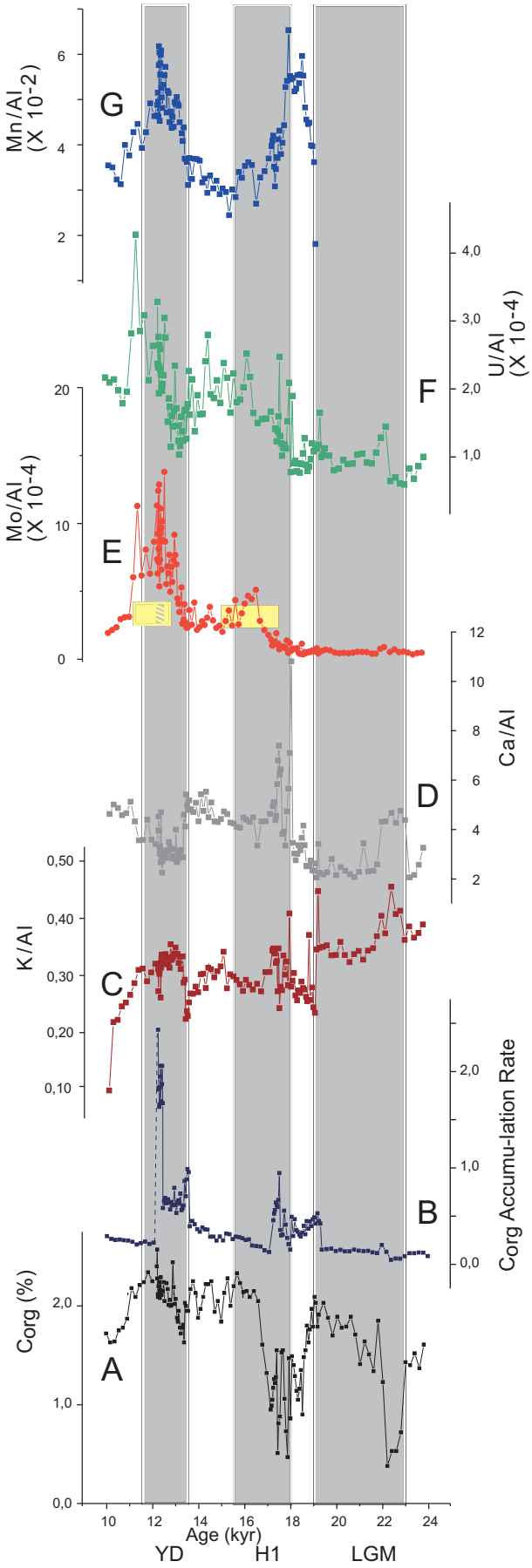

Figure 2: C_{org} (A) and Accumulation Rate (B) profiles. K/Al (C) and Ca/Al (D) used as detrital vs. carbonate sediment supply. Redox sensitive elements; Mo/Al (E) and U/Al (F) evidence reducing environment. Yellow boxes highlight AMOC collapse evidenced by *McManus et al.* 2004. Yellow-grey bar indicates reventilation event described by *Thornalley et al.* 2011.Mn/Al (G) marks diagenetic oxidation fronts. LGM: Last Glacial Maximum; HE1: Heinrich Event 1; B-A: Bolling-Allerod; YD: Younger Dryas

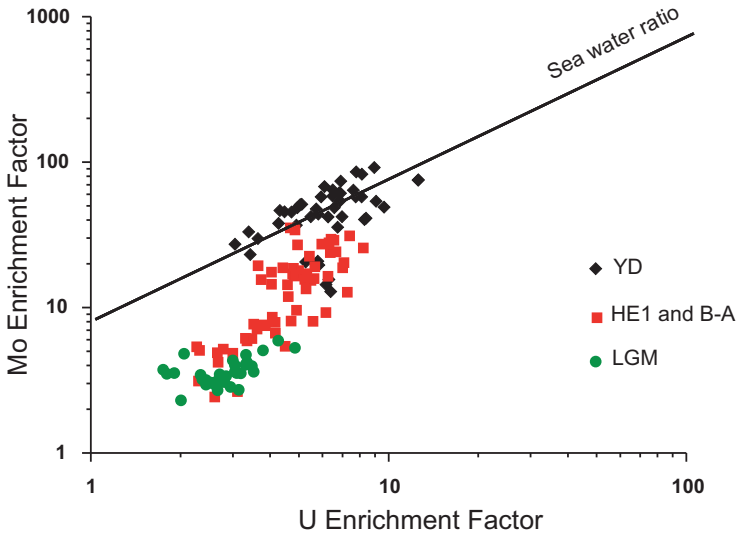

Figure 3: Mo to U covariation for three time intervals relative to average sea water composition at GeoB7926-2 (off Mauritania, NW Africa). Average sea water ratio by *Algeo and Tribovillard*, 2009.
LGM: Last Glacial Maximum; HE1: Heinrich Event 1; B-A: Bolling-Allerod; YD: Younger Dryas

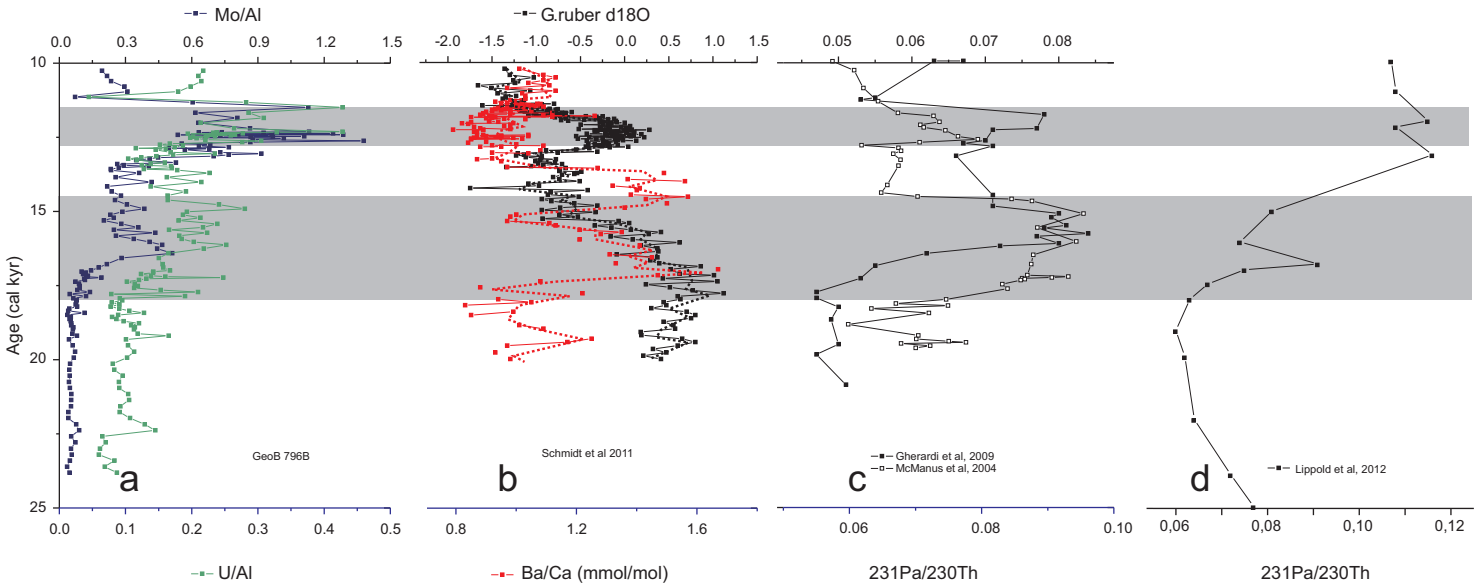

Figure 4. Comparison of redox proxies at site GeoB7926 (a), and circulation proxies in Western-most Atlantic (b), Central and Eastern North Atlantic (c), and Eastern Equatorial Atlantic (d).